REKAYASA 23 (1) (2025): 1-16

REKAYASA

Jurnal Penerapan Teknologi dan Pembelajaran

http://journal.unnes.ac.id/journals/rekayasa

# Optimization of Water-in-Biodiesel Emulsification of Palm Oil by Ultrasonic Method using Respons Surface Methodology

Dinda Adelia Fauzi[1]*, Ratna Dewi Kusumaningtyas[1], Catur Rini Widyastuti[1], Harumi Veny[2]

[1]Chemical Engineering Study Program, Universitas Negeri Semarang, Semarang, Indonesia
[2]Chemical Engineering Study Program, Universiti Teknologi Mara, Selangor, Malaysia

*Email: fauziadeliadinda@students.unnes.ac.id

**DOI:** https://doi.org/10.15294/rekayasa.v23i1.31831

**Abstract**

Palm oil biodiesel offers a renewable alternative but has high viscosity and density. Emulsifying biodiesel with water reduces these drawbacks and lowers nitrogen oxide (NOx) emissions. This study aims to optimize the emulsification process of water-in-biodiesel emulsion made from palm biodiesel (B100) using an indirect ultrasonic method and the response surface methodology approach with a Box-Behnken design. Three main independent variables were examined: hydrophilic-lipophilic balance values (6, 7.5, and 9), water concentrations (9%, 12%, and 15% v/v), and surfactant concentrations (5%, 7%, and 9% v/v) with a combination of Tween 80 and Span 80 as surfactants. The experimental process involves the synthesis of biodiesel from palm oil through transesterification with the help of 100W ultrasonic power for 15 minutes at room temperature. The analysis was carried out on three main parameters: density, viscosity, and water droplet size on water-in-biodiesel. The results of laboratory tests and statistical modeling show the three independent variables have a significant effect on the physical properties of water-in-biodiesel. The optimization resulted in the best conditions at a hydrophilic-lipophilic balance value of 6.11, water concentration of 9.06%, and surfactant concentration of 5%, with density characteristics of 859.95 kg/m$^3$, kinematic viscosity of 4.44 mm$^2$/s, and average water particle size of 4.46 μm, values close to conventional diesel fuel standards. This study confirms that the indirect ultrasonic method and respons surface methodology-based optimization are effective in improving the performance and character of water-in-biodiesel, potentially becoming a reference for the development of environmentally friendly renewable energy based on palm oil.

Keywords: energy, fossil fuels, renewable alternative, transportation, transesterification.

## INTRODUCTION

Fossil fuels have long been the primary source of energy worldwide, especially dominating the transportation sector (Maawa et al., 2020). However, their limited reserves and dependence on geopolitical factors pose

significant risks to energy security, particularly in countries like Indonesia where oil consumption surpasses domestic production for about 1.5-million-barrel oil consumption a day with 700,000-800,000 barrel per day oil produced (Sa'adah et al., 2017). The Oil Peaking Theory predict that fossil fuel will be depleted and soon diminish, creating an energy crisis that could led into economic collapse (Kreps, 2020). Furthermore, the combustion of fossil fuels substantially contributes to greenhouse gas emissions, accelerating global climate change (Kumar et al., 2019).

Renewable energy sources have thus become vital to ensuring sustainable energy supply and environmental preservation (Latisya, 2022). Among these alternatives, biodiesel derived from palm oil stands out due to its renewability and potential to reduce harmful emissions through carbon sequestration (Xu et al., 2022). Recently, the use of electric vehicles has become widespread in the transportation sector. However, due to their higher cost compared to conventional fuel-powered vehicles, the public still faces difficulties in accessing electric vehicles (Kurniawan, 2024). Consequently, this approach is considered ineffective in reducing greenhouse gas emissions (Alanazi, 2023). Furthermore, many power plants in Indonesia continue to rely on fossil fuels, particularly coal (Kurniawan, 2024). In the transportation sector, fossil fuels can be replaced with alternative fuels such as bioethanol (Bušić et al., 2018), organic oils (Sharma et al., 2019), and biodiesel (PC Lai, 2014). Biodiesel is a renewable energy product capable of replacing diesel due to its high cetane number, high oxygen content, low emissions, and low sulfur content (Maawa et al., 2020). Biodiesel is generally produced through the transesterification of organic oils with alcohol (Chasos et al., 2013). There are two method for producing biodiesel based on the impurities of Free Fatty Acid in the raw material organic oil. First method is single stage where only transesterification is required to produced FAME. The double stage method is contains of esterification using sulfuric acid catalyst, then followed by transesterification process. Single stage required to ensure that the reaction occurs towards the desired yield (Hsiao et al., 2022). The material used in this study is RBD Palm Oil thus the impurities is minimum and double stage weren't necessary (Lestari et al., 2024). Methanol were used because it contains less carobon emission and yield greater than ethanol or any other alcohol (Tangviroon & Svangariyaskul, 2014). The feedstock for biodiesel depends on regional availability, as it accounts for approximately 75% of production costs (Mahlia et al., 2020).

In Europe, commonly used as biodiesel raw material is organic oils include rapeseed oil and sunflower oil (Bickel, 2012), in China, canola oil and soybean oil are prevalent (Fan & Eskin, 2012), New Zealand and Australia predominantly use animal fats (Biermann et al., 2011), and the United States primarily uses soybean oil (PC Lai, 2014). Indonesia is one of the world's largest producers of palm oil, boasting large production capacity and competitive prices (Husin et al., 2023). Consequently, this study uses palm oil as the feedstock for biodiesel esterification. Nevertheless, biodiesel's relatively high NOx emission compared to conventional diesel can negatively impact engine performance and longevity (Ogunkule & Ahmed, 2021).

To address these challenges, emulsification of biodiesel with water (water-in-biodiesel emulsion or WiBE) has been proposed as an effective method to improve fuel properties and reduce nitrogen oxide (NOx) emissions during combustion, the existing study had been conducted of B5 Biodiesel and water, the surfactant used were

Tween 80 and Span 85, it had resulted in stable emulsion (Karim et al., 2020). This study focuses on optimizing the emulsification process of WiBE using biodiesel from palm oil (B100) via an indirect ultrasonic method combined with Response Surface Methodology (RSM) and a Box-Behnken design. By investigating the effects of key variables — surfactant Hydrophilic-Lipophilic Balance (HLB), water concentration, and surfactant concentration — this research aims to enhance the physical properties of WiBE to meet diesel fuel standards, contributing to the advancement of renewable energy technologies.

Biodiesel emulsification involves mixing water with biodiesel using surfactants, which stabilize the emulsion by reducing surface tension between oil and water (Karim et al., 2021). Common surfactants include non-ionic Polyglycerol Polyricinoleat with an HLB of 4, and Raw Karanja Oil (RKO) with an HLB of 8, although RKO is less economical due to limited raw material and high cost (Gowrishankar & Krishnasamy, 2023). Biosurfactants like lecithin and cocamide require large amounts for stability, increasing viscosity and density (Ali et al., 2024). Optimal HLB values depend on biodiesel composition; for B5 blends, HLB 7-8 is ideal, while B30 blends require HLB 6. This study uses B100 with Tween 80 and Span 80 surfactants for cost-effectiveness and availability.

High-speed mixing ensures uniform particle distribution and stable emulsions (Damayani et al., 2021). Mechanical mixers like high-shear mixers produce non-uniform droplet sizes, affecting emulsion density, viscosity, and stability (Silva et al., 2016). Colloid mills suit high-viscosity solutions (Baker & Bertola, 2018), while membrane emulsification reduces droplet size but requires frequent membrane changes and longer processing times (Güell et al., 2016). Ultrasonic emulsification offers uniform droplet size by generating cavitation bubbles through ultrasonic waves, enhancing oil-water contact and reducing emulsification time (Karim et al., 2020; Priscilla et al., 2024).

Process optimization is essential to tailor B100 emulsion characteristics for diesel engine use. RSM, especially Box-Behnken Design (BBD), is preferred for handling defined upper and lower limits on water concentration (9%-15% v/v), aligning with European Committee for Standardization guidelines. BBD offers higher efficiency than Central Composite Design for this application (Chollom et al., 2019). In Indonesia, regulations limit water content in B100 to 500 ppm, but no such rules yet exist for biodiesel emulsions. Hence, this study can be potentially becoming a reference for the development of regulation for Biodiesel emulsion.

## METHOD

The research were carried out using Aqua distilled and Commercial RBD (Refined, Bleached, and Deodorized) Palm Oil was locally purchased, the catalyst used is 0,87% Sodium hydroxide, Tween 80, and Methanol from Merck. Surfactant Span 80 from Sigma-Aldrich. The RSM Optimization used was from Statistical Software Design-Expert 25.0.2.0. The DoE was taken place before the experiment begin, using the upper level, centre point, and lower lever for determining the factors and number of runs shown in Table 1 and Table 2.

### Transesterification of RBD Palm Oil & Emulsification

The molar ratio of oil and methanol is 1:6. Reaction at 60 $^{o}$C for 2 hours and stirring at 500 rpm. After washing and evaporating the crude biodiesel, the biodiesel was then used to be emulsified using ultrasonic bath at 100W, 28 Hz, for 15 minutes.

**Table 1**. Factors Determination using Box-Behnken Design

| Factors | Lower Level (-1) | Centre Point (0) | Upper Level (+1) |
|---|---|---|---|
| HLB Value | 6 | 7.5 | 9 |
| Concentration of water (%v/v) | 9 | 12 | 15 |
| Concentration of Surfactant (%v/v) | 5 | 7 | 9 |

**Table 2**. Factors of DoE

| Run | HLB Value | Water Concentration (%) | Surfactant Concentration (%) |
|---|---|---|---|
| 1 | 7.5 | 12 | 7 |
| 2 | 7.5 | 15 | 5 |
| 3 | 7.5 | 12 | 7 |
| 4 | . | 9 | 7 |
| 5 | 9 | 15 | 7 |
| 6 | 7.5 | 12 | 7 |
| 7 | 6 | 12 | 9 |
| 8 | 7.5 | 9 | 9 |
| 9 | 7.5 | 9 | 5 |
| 10 | 6 | 15 | 7 |
| 11 | 7.5 | 12 | 7 |
| 12 | 7.5 | 12 | 7 |
| 13 | 9 | 9 | 7 |
| 14 | 9 | 12 | 9 |
| 15 | 6 | 12 | 5 |
| 16 | 9 | 12 | 5 |
| 17 | 7.5 | 15 | 9 |

The transesterification of RBD Palm oil was performed at molar ratio of oil and methanol 1:6. Reaction at 60 °C for 2 hours and stirring at 500 rpm. After washing and evaporating the resulted biodiesel, it was then used to be emulsified after adding the surfactants and water according to DoE, using ultrasonic bath at 100W frequency at 28 Hz for 15 minutes.

**Determination of Density**

Biodiesel and WiBE densities were measured and compared with conventional diesel products. Density measurements were conducted using a pycnometer. The density is calculated using Equation (1).

$$\rho = \frac{m\ pycnometer\ with\ content - m\ pycnometer\ empty}{V\ pycnometer} \quad (1)$$

**Determination of Viscosity**

The viscosity of WiBE was measured using an Ostwald viscometer to determine its dynamic viscosity. The parameters used were the viscosity and density of distilled water. The dynamic viscosity is calculated using Equation (2).

$$\mu = \mu \frac{t \times \rho}{t_0 \times \rho_0} \quad (2)$$

Kinematic viscosity can be calculated by dividing the dynamic viscosity by the density shown in Equation (3).

$$v = \frac{\mu}{\rho} \quad (3)$$

**Determination of Particle size**

Particle size measurement of emulsions can be performed using the Cilas 1090 Laser Diffraction Liquid instrument. This instrument detects a range of particle sizes within a sample and calculates the Mean Diameter based on their distribution percentages. The particle size distribution is divided into three parts: D10, D50, and D90. The measurement results are automatically obtained. The mean diameter is calculated using Equation (4).

$$D = \frac{\sum di \times fi}{\sum fi} \quad (4)$$

**Optimization using Response Surface methodology**

After the dependent variable data (response) is known, the data undergoes quadratic regression analysis to map the relationship between independent variables and the response. The next statistical analysis to test the significance of each variable's model involves analysis of variance (ANOVA) to ensure that the resulting model is valid and can

be used for prediction. The results are visualized by creating Contour Plots and Response Surface Plots to illustrate the interactions among variables and to assist in identifying the optimal conditions of the emulsification process.

## RESULT AND DISCUSSION

### WiBE Characteristic

The highest density is found in samples 7 and 8, with a density value of 866 kg/m³ shown in Figure 1. The lowest density, 859 kg/m³, is observed in sample 9. The desired density range is between 820 and 860 kg/m³ based on the density of Pertamina Dex. The highest density is undesirable in this study, since it could cause the nozzle of ignition chamber to be clogged. Therefore, samples 2, 3, 6, and 9 meet the required criteria. The highest kinematic viscosity was observed in sample 7, with a value of 5.15 mm²/s shown in Figure 2. The lowest viscosity was recorded in sample 16, at 4.36 mm²/s. The desired viscosity range is between 2 and 4.5 mm²/s, according to the viscosity of Pertamina Dex. Therefore, samples 2, 6, and 16 meet the specified criteria. The smallest particle size of WiBE was 5.8 μm in sample 5, while the largest was 12.15 μm in sample 2 shown in Figure 3. In this study, the desired response was the minimum particle size; therefore, sample 5 met the criteria.

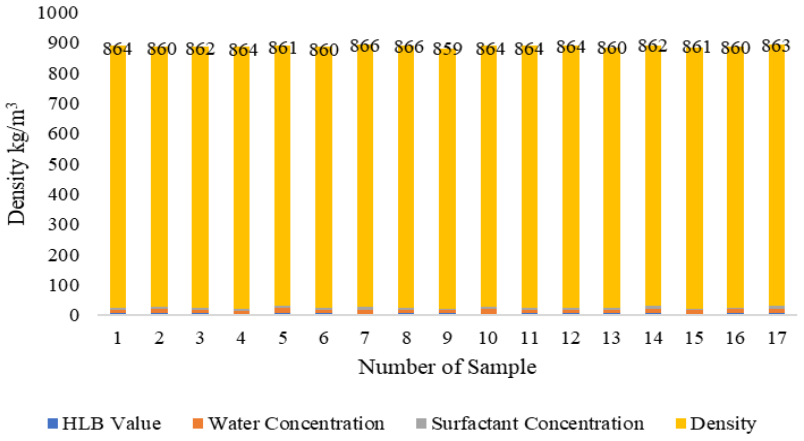


**Figure 1**. Density of WiBE

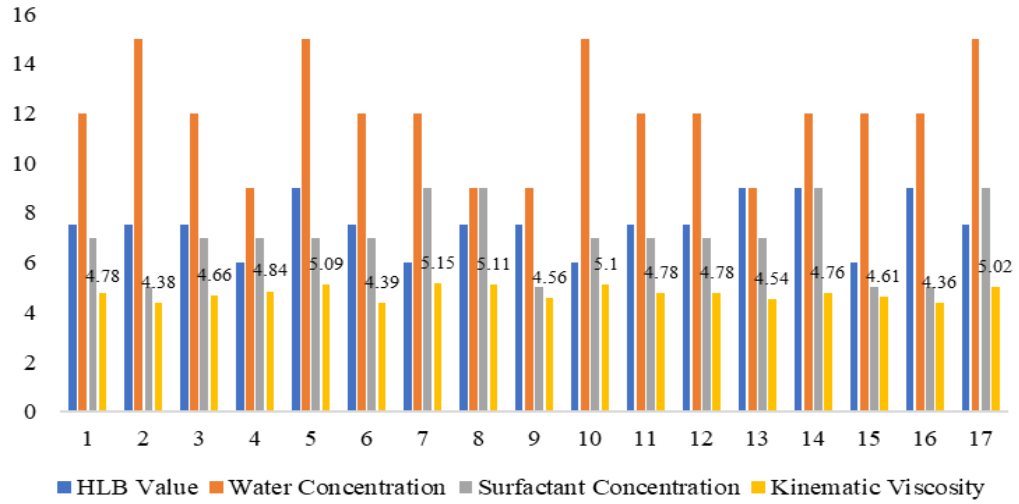


**Figure 2**. Viscosity of WiBE

**Response Mathematical Model**

Based on the simulation conducted using Design Expert, a mathematical equation to predict the response value was obtained. For the density response, a linear ANOVA model was used with an F-value of 10.35. Table 3, indicating the model is significant. The lack of fit p-value was 0.97 (p-value >0.05) and not significant, confirming the model's suitability (Rengga et al., 2022).

The predicted coefficient of determination (Predicted $R^2$) is 0.64, and the adjusted coefficient of determination (Adjusted $R^2$) is 0.7. The difference between these values is less than 0.2, indicating that the model and design are acceptable although can not be used to predict new data. The Adequate Precision value of 11.44 signifies a strong signal-to-noise ratio, with an ideal value being greater than 4. Therefore, this regression model has a sufficiently strong signal compared to the variation or noise in data shown in Figure 4.

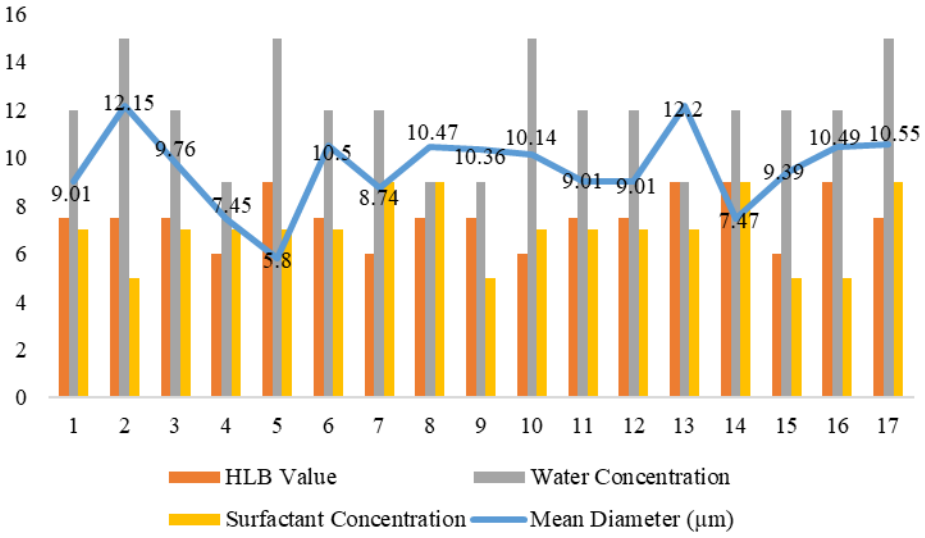


**Figure 3**. Particle Size of WiBE

**Table 3**. ANOVA Linear Model for Response 1 (Density)

| Source | Sum of Squares | df | Mean Square | F-value | p-value |
|---|---|---|---|---|---|
| **Model** | 60.38 | 4 | 15.09 | 10.35 | 0.0007 significant |
| A-HLB Value | 18.00 | 1 | 18.00 | 12.34 | 0.0043 |
| C-Concentration (v/v) | 36.13 | 1 | 36.13 | 24.76 | 0.0003 |
| AC | 2.25 | 1 | 2.25 | 1.54 | 0.2380 |
| BC | 4.00 | 1 | 4.00 | 2.74 | 0.1237 |
| **Residual** | 17.51 | 12 | 1.46 | | |
| Lack of Fit | 4.71 | 8 | 0.5884 | 0.1839 | 0.9795 not significant |
| Pure Error | 12.80 | 4 | 3.20 | | |
| **Cor Total** | 77.88 | 16 | | | |

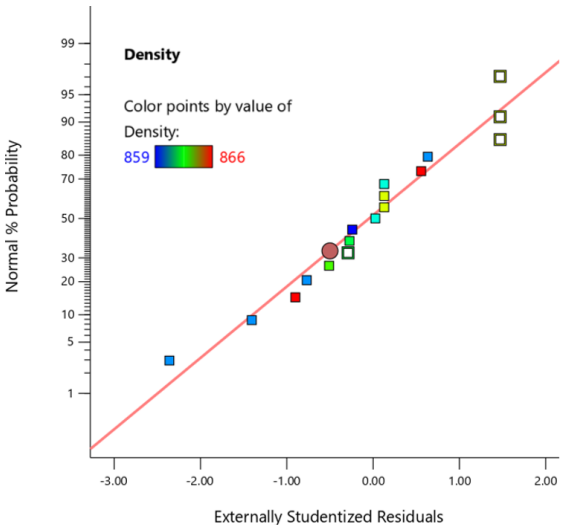


**Figure 4**. Density Normal Plot of Residuals

Total Variance Inflation Factor (VIF) value of 3, which is within the acceptable limit of less than 10 shown in Table 4. The mathematical equation to predict the density value in this study is as Equation (5).

$$y1 = 862{,}35 - 1{,}5A + 2{,}13C - 0{,}75AC - BC \quad (5)$$

where A is HLB Value, B symbolic for water concentration (v/v%), and C is for surfactant concentration.

Based on the simulation conducted using Design Expert, a mathematical equation to predict the response value was obtained. For the particle size response, a linear ANOVA model was used with an F-value of 43.71 as shown in Table 5.

**Table 4**. Coefficient and Mathematical Model of Response 1 (Density)

| Factor | Coefficient Estimate | df | Standard Error | 95% CI Low | 95% CI High | VIF |
|---|---|---|---|---|---|---|
| Intercept | 862.35 | 1 | 0.2930 | 861.71 | 862.99 | |
| A-HLB Value | -1.50 | 1 | 0.4270 | -2.43 | -0.5695 | 1.0000 |
| C-Concentration (v/v) | 2.13 | 1 | 0.4270 | 1.19 | 3.06 | 1.0000 |
| AC | -0.7500 | 1 | 0.6039 | -2.07 | 0.5659 | 1.0000 |
| BC | -1.0000 | 1 | 0.6039 | -2.32 | 0.3159 | 1.0000 |

**Table 5**. ANOVA Quadratic Model for Response 2 (Particle Size)

| Source | Sum of Squares | df | Mean Square | F-value | p-value | |
|---|---|---|---|---|---|---|
| Model | 737.98 | 7 | 105.43 | 43.71 | < 0.0001 | significant |
| AB | 20.66 | 1 | 20.66 | 8.56 | 0.0169 | |
| BC | 153.02 | 1 | 153.02 | 63.43 | < 0.0001 | |
| $A^2$ | 93.11 | 1 | 93.11 | 38.60 | 0.0002 | |
| $B^2$ | 59.84 | 1 | 59.84 | 24.81 | 0.0008 | |
| $C^2$ | 63.88 | 1 | 63.88 | 26.48 | 0.0006 | |
| $B^2C$ | 155.75 | 1 | 155.75 | 64.57 | < 0.0001 | |
| $BC^2$ | 200.51 | 1 | 200.51 | 83.12 | < 0.0001 | |
| Residual | 21.71 | 9 | 2.41 | | | |
| Lack of Fit | 8.26 | 5 | 1.65 | 0.4915 | 0.7723 | not significant |
| Pure Error | 13.45 | 4 | 3.36 | | | |
| Cor Total | 759.69 | 16 | | | | |

indicating the model is significant (Rengga et al., 2022). The lack of fit p-value was 0.7723 (>0.05) and not significant, confirming the model's appropriateness. The coefficient of determination ($R^2$) is 0.97, showing that the prediction is similar with the data as shown in Figure 5. Therefore, this equation can be used. The mathematical equation to predict the particle size value in this study is as Equation (6).

$$y2 = 9{,}83 - 2{,}27AB + 6{,}18BC - 4{,}7A^2 + 3{,}77B^2 + 3{,}9C^2 + 6{,}24B^2C + 7{,}08BC^2 \quad (6)$$

Based on the simulation conducted using Design Expert, a mathematical equation to predict the response value was obtained. For the viscosity response, a linear ANOVA model was used with an F-value of 12.96 (p-value = 0.0003) shown in Table 6, indicating the model is significant. The lack of fit p-value was 0.7678 and not significant, confirming the model's appropriateness (Rengga et al., 2022). The predicted coefficient of determination (Predicted $R^2$) is 0.52, and the adjusted coefficient of determination (Adjusted $R^2$) is 0.69. The difference between the two is lss than 0.2, indicating that the model and design are acceptable. An Adequate Precision value of 10.77 indicates a strong signal-to-noise ratio, with an ideal value being greater than 4. Therefore, this regression model has a sufficiently strong signal compared to the variation or noise present in the data shown in Figure 6. The total Variance Inflation Factor (VIF) value is 3, which is within the tolerable limit of less than 10; therefore, this equation can be used. The mathematical equation to predict the viscosity value in this study is as Equation (7).

$$y3 = 4{,}77 - 0{,}079A + 0{,}2663B + 0{,}2025A^2B \quad (7)$$

**Effect of HLB Value on the Response**

It is observed that as the HLB value of the surfactant increases, the density of WiBE decreases shown in Figure 7. Higher HLB values result in lighter and less dense emulsion structures because high HLB indicates greater hydrophilicity, allowing the emulsion to hold more water particles. Additionally, surfactant molecules with high HLB tend to form thicker layers between water particles, creating larger intermolecular spaces and reducing mixture density.

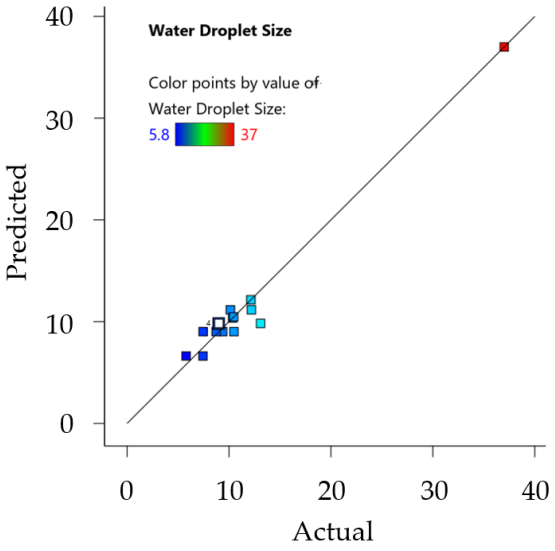


**Figure 5**. Water Droplet Size Data Predicted vs. Actual

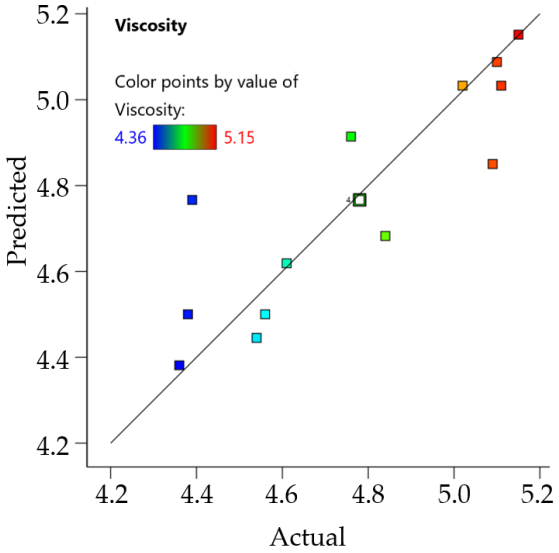


**Figure 6**. Viscosity Predicted Data vs. Actual

High HLB surfactants are generally suited for oil-in-water emulsions, whereas biodiesel, being a water-in-oil emulsion, is more compatible with low HLB surfactants. This aligns with research showing that low HLB values form thinner water-oil molecular structures, resulting in higher density compared to emulsions with higher HLB surfactants (Wang et al., 2023).

Based on Figure 8, the water particle size in WiBE initially increases with rising HLB values, reaches a peak, and then decreases. This occurs because low HLB values are suitable for water-in-biodiesel emulsions. Higher HLB values cause oil particles to self-emulsify into smaller particles with surrounding water flocculation, resulting in a reduction of the mean particle diameter after the flocculation point is reached (Park & Kim, 2021).

**Table 6**. ANOVA Linear Model for Response 3 (Viscosity)

| Source | Sum of Squares | df | Mean Square | F-value | p-value | |
|---|---|---|---|---|---|---|
| **Model** | 0.8439 | 3 | 0.2813 | 12.96 | 0.0003 | significant |
| A-HLB Value | 0.1128 | 1 | 0.1128 | 5.20 | 0.0402 | |
| C-Concentration (v/v) | 0.5671 | 1 | 0.5671 | 26.12 | 0.0002 | |
| $A^2B$ | 0.1640 | 1 | 0.1640 | 7.56 | 0.0166 | |
| **Residual** | 0.2822 | 13 | 0.0217 | | | |
| Lack of Fit | 0.1606 | 9 | 0.0178 | 0.5864 | 0.7678 | not significant |
| Pure Error | 0.1217 | 4 | 0.0304 | | | |
| **Cor Total** | 1.13 | 16 | | | | |

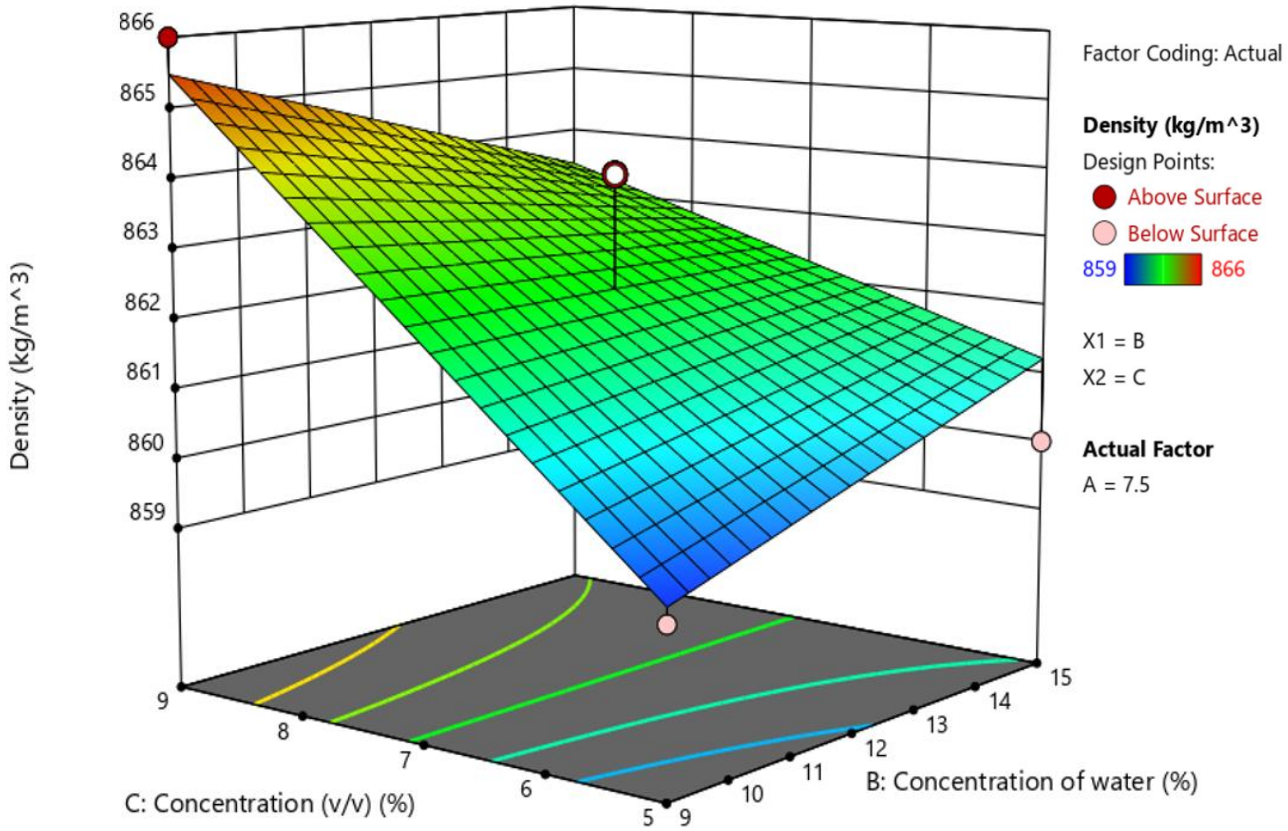


**Figure 7**. Graphs of Density on Factors

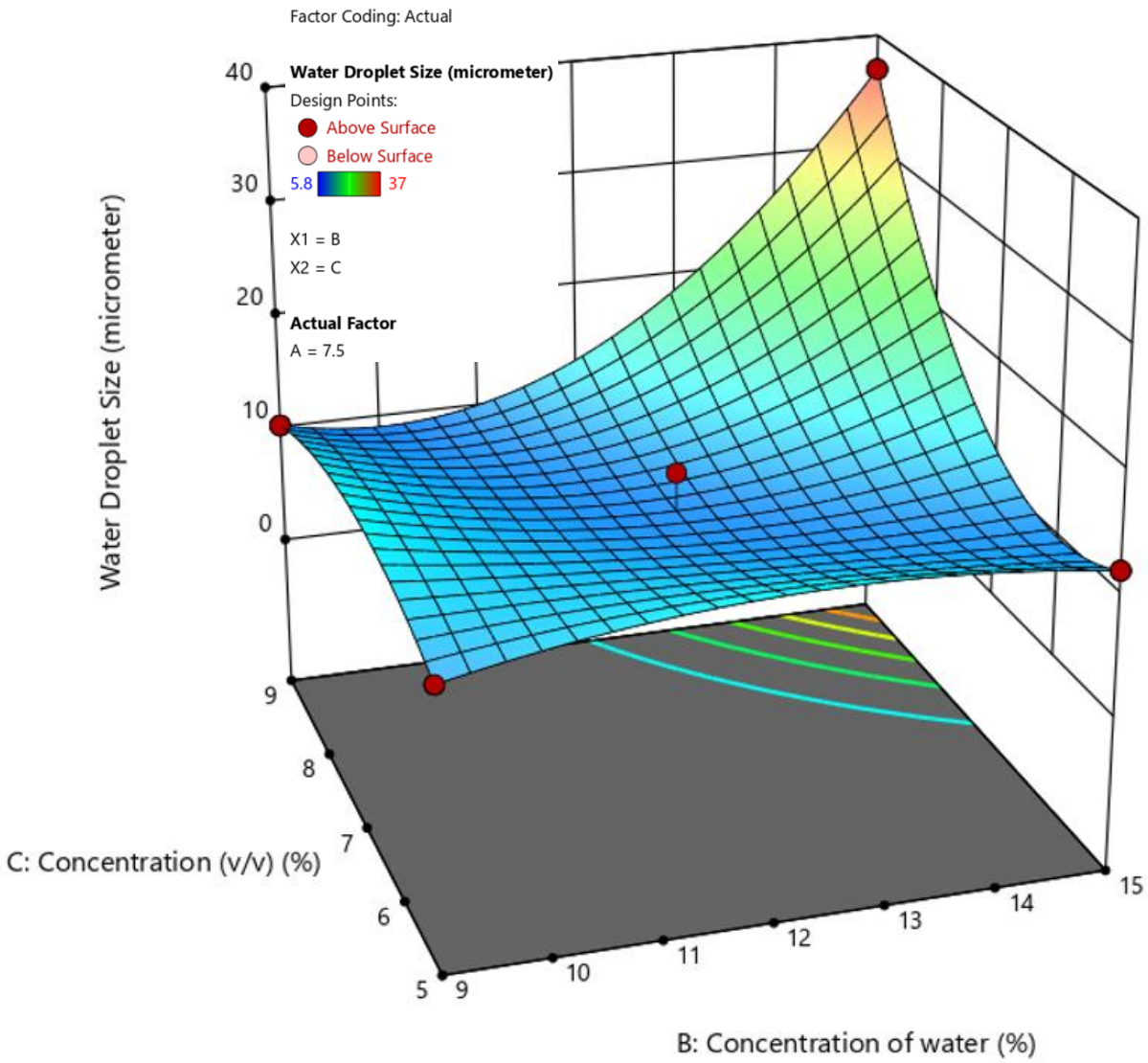


**Figure 8**. Graphs of Particle Size on Factors

Increasing the HLB value reduces the viscosity of WiBE, with viscosity changes becoming less significant after reaching an optimal point shown in Figure 9. Higher HLB values indicate more lipophilic surfactants and larger water particle sizes in oil, affecting viscosity due to inter-particle cohesion and emulsified oil phase reducing cohesion (Damayani et al., 2021). In this study, emulsification was used to lower viscosity for more efficient fuel atomization. High HLB surfactants reduce interfacial cohesion, resulting in lower attractive forces between particles (Fang et al., 2022).

**Effect of Water Concentration on the Response**

The emulsion density increases until reaching equilibrium, then decreases as water concentration rises. The highest density occurs at 12% water, dropping at 15%. This is influenced by factors such as the HLB value. The highest density at the combination of the lowest HLB value and lowest water concentration, as more lipophilic surfactants cannot retain water effectively shown in Figure 7. This aligns with research indicating that water concentration affects the density of

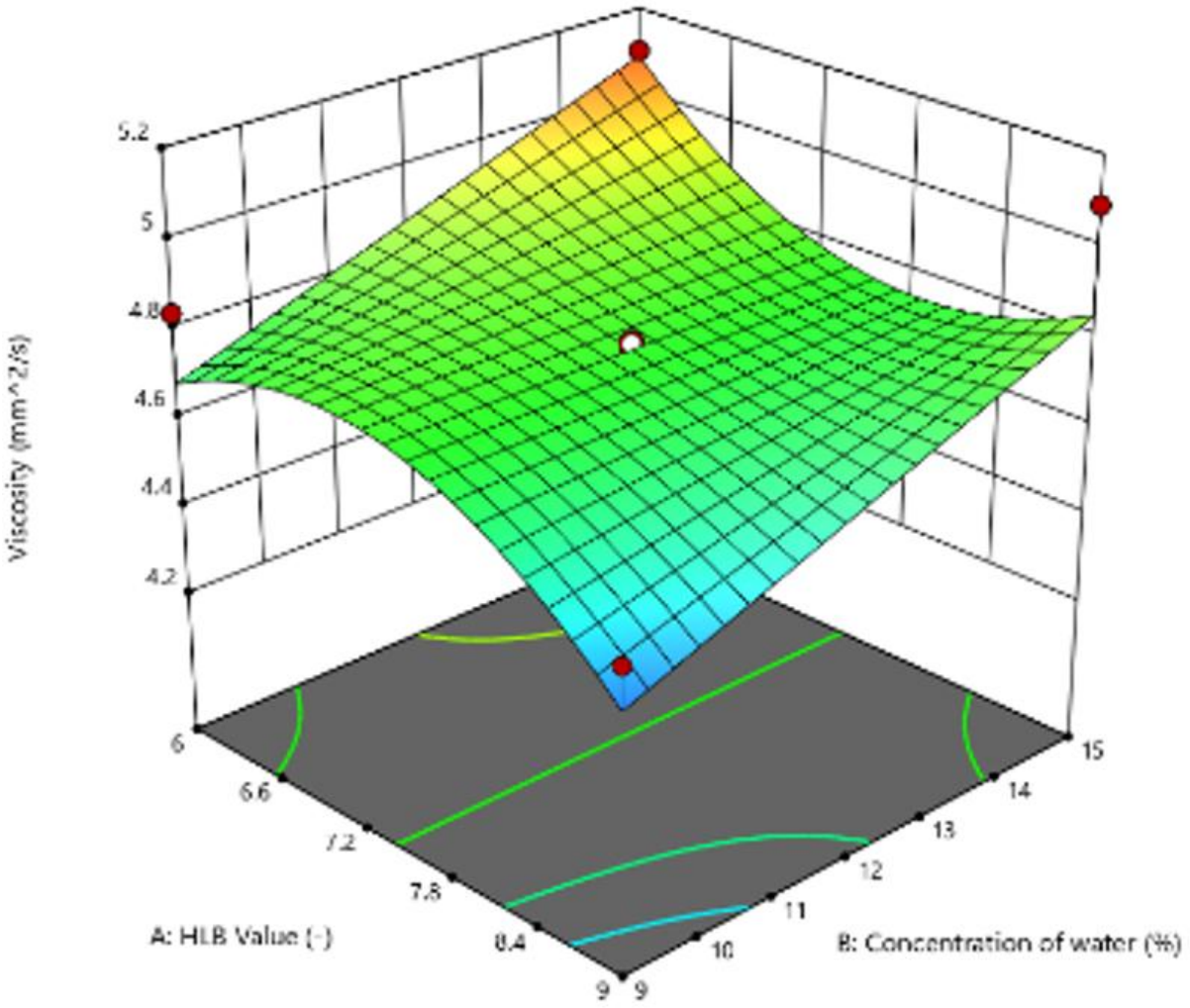


**Figure 9**. Graphs of Viscosity on Factors

water-in-oil emulsions (Sagdeev et al., 2023).

The water particle size decreases from 10 μm to 9 μm as concentration rises from 9% to 12%, then increases again at 15% shown in Figure 11. This occurs because higher water concentration reduces the oil phase ratio and particle size, but after reaching the minimum size, water particle flocculation causes the mean diameter to increase (Pérez et al., 2016). The decrease in viscosity is due to the reduction of inter-particle oil tension caused by the dispersed water phase, which reduces the dispersion forces between particles and lowersviscosity. The minimum point is reached when the concentration of the dispersed phase (water) becomes saturated in the system shown in Figure 9, leading to coalescence. This causes water particles to merge into larger particles, increasing the interfacial surface tension and subsequently raising the emulsion's viscosity.

**Effect of Surfactant Concentration on the Response**

The relationship between density and surfactant concentration shows a positive correlation, where the density increases with the addition of surfactant concentration in the emulsion shown in Figure 7. It is evident that the increase in surfactant concentration linearly raises the density in WiBE, as surfactants enhance the surface tension of water. Therefore, a high surfactant concentration promotes flocculation in the emulsion due to the reduction of the energy barrier between

molecules, which in turn increases molecular packing density (Ravera et al., 2021). The increase in surfactant concentration causes a rise in viscosity shown in Figure 9. This is due to the surfactant's ability to form a thicker interfacial layer between water particles in oil as a result of the reduction in the energy barrier by the surfactant. Consequently, the dispersion forces between the particles become stronger, leading to an increase in the system's viscosity Ravera et al., 2021). The increase in surfactant concentration shows a decrease in particle size; however, after reaching a minimum point, further increases in surfactant concentration no longer affect the particle size in the emulsion system shown in Figure 15. This occurs because the system has reached the Critical Micelle Concentration (CMC). Under this condition, the entire water-particle interface is fully covered by surfactant molecules, so the addition of more surfactant does not lead to a reduction in particle size. One of the kind surfactant molecules in general that cannot bind to water will form aggregates such as micelles (Chagot et al., 2022). The summarizes the comparation between WiBE and Diesel characteristic shown in Table 7.

**Optimization for Emulsification of B100 WiBE**

It was found that the best regression model is the quadratic model with $R_i^2$ values approaching 0 and 0, indicating that all terms are correlated with each other shown in Table 8. The Variance Inflation Factor (VIF) is a measure used in multicollinearity tests within regression models to detect linear dependence among variables. The ideal value is 1; therefore, in this study, the coefficients used are appropriate to represent the derived mathematical model. The lack of fit value is 3 and the pure error is 4, which are the maximum allowable values for the lack of fit test to be valid. The optimization solutions generated by the simulation total 73 solutions. In this study, 56 optimization solutions were identified to obtain WiBE characteristics comparable to those of conventional diesel. Desirability indicates the optimality of a solution; the closer the value is to 1, the more optimal the solution is considered (Kusumaningtyas et al., 2022). The highest desirability value is 1 at solution number 1 shown in Figure 10. Based on this solution, with an HLB value of 6.11, water concentration of 9.06%, and surfactant concentration of 5%, the predicted responses are a density of 859.95 kg/m$^3$, a particle size of 4.46 μm, and a viscosity of 4.44 mm$^2$/s.

**Table 7.** Comparation of WiBE and Diesel

| Component | WiBE | Diesel |
|---|---|---|
| **Viscosity** | **2.3 – 6 mm$^2$/s** | **2 – 4.5 mm$^2$/s** |
| **Density** | **860 – 900 kg/m$^3$** | **820 – 860 kg/m$^3$** |

**Table 8.** Optimization Model

| Term | Standard Error* | VIF | $R_i^2$ | Power |
|---|---|---|---|---|
| A | 0.3536 | 1 | 0.0000 | 68.1% |
| B | 0.3536 | 1 | 0.0000 | 68.1% |
| C | 0.3536 | 1 | 0.0000 | 68.1% |
| AB | 0.5000 | 1 | 0.0000 | 40.8% |
| AC | 0.5000 | 1 | 0.0000 | 40.8% |
| BC | 0.5000 | 1 | 0.0000 | 40.8% |
| $A^2$ | 0.4873 | 1.00588 | 0.0058 | 93.8% |
| $B^2$ | 0.4873 | 1.00588 | 0.0058 | 93.8% |
| $C^2$ | 0.4873 | 1.00588 | 0.0058 | 93.8% |

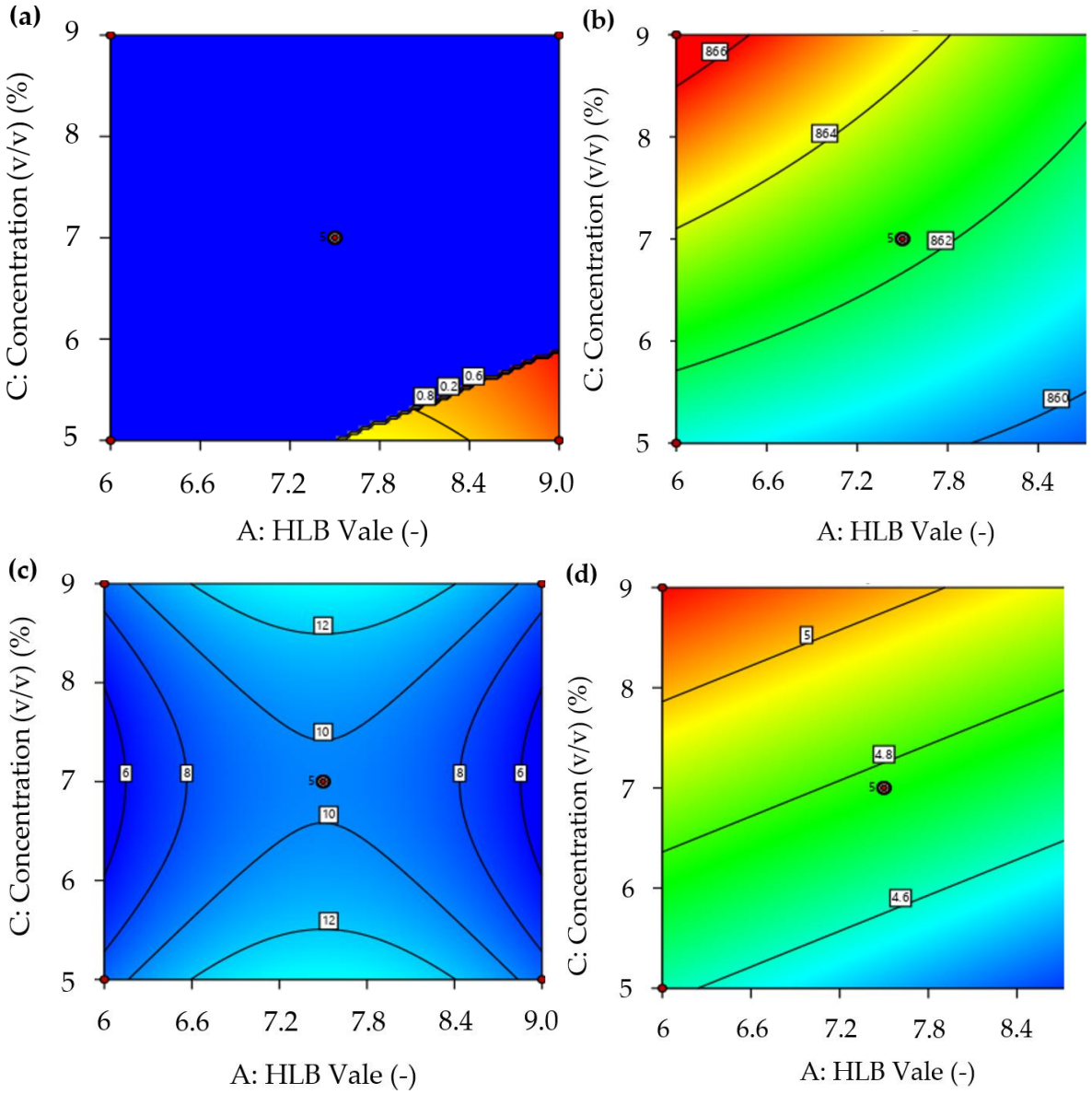


**Figure 10**. Optimization of WiBE of: (a) Desireability; (b) Density, kg/m³; (c) Water droplet size, μm; and (d) Viscosity, mm²/s. Factor Coding: Actual; Std # 17 Run # 1; X1 = A = 7.5; X2 = C = 7; Actual Factor = B = 12.

## CONCLUSION

This study demonstrated that the physical properties—density, viscosity, and water droplet size—of water-in-palm oil biodiesel emulsions (WiBE) can be significantly optimized using an indirect ultrasonic method combined RSM and a Box-Behnken Design. The research identified the optimal emulsion conditions at an HLB value of 6.11, water concentration of 9.06%, and surfactant concentration of 5%. Under these optimal conditions, the WiBE exhibited desirable physical characteristics: a density of 859.95 kg/m³, kinematic viscosity of 4.46 mm²/s, and average water droplet size of 4.44 μm. These results closely match the standards for conventional diesel fuel, supporting the practical potential of WiBE as a renewable and environmentally friendlier alternative fuel. The findings confirm that the indirect ultrasonic emulsification method is effective for

producing water-in-biodiesel emulsions with properties suited for diesel engine application and that RSM is a powerful tool for process optimization.

**REFERENCES**

Alanazi, F. (2023). Electric Vehicles: Benefits, Challenges, and Potential Solutions for Widespread Adaptation. Applied Sciences, 13(10), 6016.

Ali, A., Aziz, A. R. A., Ismael, M. A., & Alqaed, S. (2024). The investigation of lecithin and cocamide DEA Biosurfactant concentrations on emulsified biodiesel fuel stability, properties, and the micro-explosion phenomenon. Results in Engineering, 23, 102482.

Baker, T., Negri, M., & Bertola, V. (2018). Atomization of high-viscosity and non-Newtonian fluids by premixing. Atomization and Sprays, 28(5), 1-18

Bickel, S. (2012). Ölpflanzen in Europa. Biologie in Unserer Zeit, 42(4), 222–231. https://doi.org/10.1002/biuz.201210482

Biermann, U., Bornscheuer, U., Meier, M. A. R., Metzger, J. O., & Schäfer, H. J. (2011). Oils and Fats as Renewable Raw Materials in Chemistry. Angewandte Chemie International Edition, 50(17), 3854–3871.

Chagot, L., Quilodrán-Casas, C., Kalli, M., Kovalchuk, N. M., Simmons, M. J. H., Matar, O. K., Arcucci, R., & Angeli, P. (2022). Surfactant-laden droplet size prediction in a flow-focusing microchannel: a data-driven approach. Lab on a Chip, 22(20), 3848–3859.

Chasos, C. A., Karagiorgis, G. N., & Christodoulou, C. N. (2013). Diesel Internal Combustion Engine Emissions Measurements for Methanol-Based and Ethanol-Based Biodiesel Blends. In Conference Papers in Science (Vol. 2013, No. 1, p. 162312). Hindawi Publishing Corporation.

Damayani, I. A., Paramita, V., & Yulianto, M. E. (2021). The Effect of HLB Surfactant Value on The Characteristics of Emulsion Biodiesel Palm Oil Using Homogenizer. Journal of Vocational Studies on Applied Research, 3(1), 9–13.

Fan, L., & Eskin, N. A. M. (2012). Frying oil use in China. Lipid Technology, 24(6), 131–133.

Fang, Q., Zhao, X., Li, S., Qiu, Z., Wang, Z., & Geng, Q. (2022). Effect of surfactants with different hydrophilic–lipophilic balance on the cohesive force between cyclopentane hydrate particles. Journal of Marine Science and Engineering, 10(9), 1255.

Gowrishankar, S., & Krishnasamy, A. (2023). Emulsification – A promising approach to improve performance and reduce exhaust emissions of a biodiesel fuelled light-duty diesel engine. Energy, 263, 125782.

Güell, C., Ferrando, M., & Schroën, K. (2016). Membranes for enhanced emulsification processes. Innovative Food Processing Technologies, 429-453.

Hsiao, M. C., Liao, P. H., Yang, K. C., Lan, N. V., & Hou, S. S. (2022). Enhanced Biodiesel Synthesis via a Homogenizer-Assisted Two-Stage Conversion Process Using Waste Edible Oil as Feedstock. Energies, 15(23), 9036.

Husin, S., Wijaya, C., Ghafur, H. S., Mardanugraha, E., & Machmud, T. M. Z. (2023). Indonesian's Position in the World Vegetable Oil Trade. Economics Development Analysis Journal, 12(4), 472–489.

Karim, Z. A. A., Kaur, E., Masharuddin, S. M. S., Khan, M. Y., & Hagos, F. Y. (2020). The characteristics of water-in-biodiesel

emulsions produced using ultrasonic homogenizer. Alexandria Engineering Journal, 59(1), 227-237.

Kreps, B. H. (2020). The rising costs of fossil-fuel extraction: an energy crisis that will not go away. American journal of economics and sociology, 79(3), 695-717.

Kumar, A., Bhansali, S., Gupta, N., & Sharma, M. (2019). Bioenergy and climate change: greenhouse gas mitigation. In Prospects of Renewable Bioprocessing in Future Energy Systems, 10, 269-289.

Kurniawan, D. (2024). Investigating the effectivity of promoting electric vehicle to reduce air pollution: An analysis of Indonesia power plants. Journal of Law and Sustainable Development, 12(2), 2731-2731.

Kusumaningtyas, R. D., Normaliza, N., Anisa, E. D. N., Prasetiawan, H., Hartanto, D., Veny, H., Hamzah, F., & Rodhi, M. N. M. (2022). Synthesis of Biodiesel via Interesterification Reaction of Calophyllum inophyllum Seed Oil and Ethyl Acetate over Lipase Catalyst: Experimental and Surface Response Methodology Analysis. Energies, 15(20), 7737.

Latisya, S. (2022). Teknologi Proses Untuk Produksi Biodiesel Berbasis Minyak Kelapa Sawit. WARTA Pusat Penelitian Kelapa Sawit, 27(2), 78–91.

Lestari, P., Yusuf, F., & Fahdi, F. (2024). Quality analysis of cooking oil (RBD Palm Olein) based on PORAM standard specifications. Science Midwifery, 12(2), 1040-1046.

Maawa, W. N., Mamat, R., Najafi, G., & De Goey, L. P. H. (2020). Performance, combustion, and emission characteristics of a CI engine fueled with emulsified diesel-biodiesel blends at different water contents. Fuel, 267, 117265.

Mahlia, T. M. I., Syazmi, Z. A. H. S., Mofijur, M., Abas, A. E. P., Bilad, M. R., Ong, H. C., & Silitonga, A. S. (2020). Patent landscape review on biodiesel production: Technology updates. Renewable and Sustainable Energy Reviews, 118, 109526.

Ogunkunle, O., & Ahmed, N. A. (2021). Overview of biodiesel combustion in mitigating the adverse impacts of engine emissions on the sustainable human–environment scenario. Sustainability, 13(10), 5465.

Park, Y. H., & Kim, H. J. (2021). Formulation and stability of horse oil-in-water emulsion by HLB system. Food Science and Biotechnology, 30(7), 931–938.

PC Lai, E. (2014). Biodiesel: Environmental Friendly Alternative to Petrodiesel. Journal of Petroleum & Environmental Biotechnology, 05(01).

Pérez, M. P., Wagner, J. R., & Márquez, A. L. (2016). Influence of different factors on the particle size distribution and solid fat content of water-in-oil emulsions. Journal of the American Oil Chemists' Society, 93(6), 793-801.

Priscilla, T., Irwan, Muh., & Arifin, Z. (2024). Sintesis Biodiesel Dari Minyak Jelantah Dalam Reaktor Ultrasonik. Jurnal Energi Baru Dan Terbarukan, 5(1), 44–56.

Ravera, F., Dziza, K., Santini, E., Cristofolini, L., & Liggieri, L. (2021). Emulsification and emulsion stability: The role of the interfacial properties. Advances in Colloid and Interface Science, 288, 102344.

Rengga, W. D. P., Hartanto, D., Widyastuti, C. R., Permani, T. K., & Mahfudhoh, M. A. (2022). Optimization of Glycerolysis of Free Fatty Acids from Cocoa Bean with MgO Catalyst Using Response Surface Methodology. Jurnal Bahan Alam

Terbarukan, 11(2), 108–114.

Sa'adah, A. F., Fauzi, A., & Juanda, B. (2017). Peramalan Penyediaan dan Konsumsi Bahan Bakar Minyak Indonesia dengan Model Sistem Dinamik. Jurnal Ekonomi Dan Pembangunan Indonesia, 17(2), 118–137.

Sagdeev, D. I., Khairutdinov, V. F., Farakhov, M., Alyaev, V. A., Gumerov, F. M., Zaripov, Z. I., Minkin, V. S., & Abdulagatov, I. M. (2023). Measurements of the Density and Viscosity of Heavy Oil and Water-in-Oil Emulsions Over a Wide Temperature Range. International Journal of Thermophysics, 44(1), 7.

Silva, T. M., Cerize, N. N. P., & Oliveira, A. M. (2016). The Effect of High Shear Homogenization on Physical Stability of Emulsions. International Journal of Chemistry, 8(4), 52.

Tangviroon, P., & Svang-Ariyaskul, A. (2014). Life cycle assessment comparison between methanol and ethanol feedstock for the biodiesel from soybean oil (Doctoral dissertation, Sirindhorn International Institute of Technology, Thammasat University).

Wang, Q., Zhang, H., Han, Y., Cui, Y., & Han, X. (2023). Study on the relationships between the oil HLB value and emulsion stabilization. RSC Advances, 13(35), 24692–24698.

Xu, H., Ou, L., Li, Y., Hawkins, T. R., & Wang, M. (2022). Life Cycle Greenhouse Gas Emissions of Biodiesel and Renewable Diesel Production in the United States. Environmental Science and Technology, 56(12), 7512–7521.